CMS Physics Analysis Summary

Contact: cms-pag-conveners-higgs@cern.ch 2012/07/09

Evidence for a new state in the search for the standard model Higgs boson in the $H \to ZZ \to 4\ell$ channel in pp collisions at $\sqrt{s} = 7$ and 8 TeV

The CMS Collaboration

Abstract

A search for the Higgs boson in the $H \to ZZ$ four-lepton decay channel, with each Z boson decaying to an electron, a muon, or a tau pair, is reported. The search covers Higgs boson mass hypotheses in the range $110 < m_H < 600$ GeV. The analysis uses pp collision data recorded by the CMS detector at the LHC, corresponding to integrated luminosities of 5.05 fb^{-1} at $\sqrt{s}$ = 7 TeV and 5.26 fb^{-1} at $\sqrt{s}$ = 8 TeV. The four-lepton invariant-mass distributions for $m_{4\ell}$ and $m_{2\ell 2\tau}$ are found to be consistent with the standard model expectations for background ZZ production for invariant masses above 180 GeV. Upper limits at 95% confidence level exclude the standard model Higgs boson in the range 131–162 and 172–525 GeV, while the expected exclusion range is 121–570 GeV. An excess of events is observed in the low $m_{4\ell}$ mass range, making the observed limits weaker than expected in the absence of a signal. These events cluster around a mass $m_{4\ell} \simeq 125.5$ GeV, giving rise to a local excess with respect to the background expectation, with a significance of 3.2σ. This result constitutes evidence for a new massive state.

1 Introduction

The standard model (SM) of electroweak interactions [1–3] relies on the existence of the Higgs boson (H), a scalar particle of mass m_{H} associated with the field responsible for the spontaneous electroweak symmetry breaking [4–9]. The value of m_{H} is not fixed by the theory, and the existence of the scalar boson has not yet been established experimentally. The production of a Higgs boson, followed by its decay $\mathrm{H} \to \mathrm{ZZ}$, is expected to be one of the main discovery channels at the proton-proton (pp) Large Hadron Collider (LHC) [10] for a wide range of m_{H} values.

Direct searches for the SM Higgs bosons have been performed by the ATLAS and CMS experiments using each about 5 fb^{-1} of pp data from the LHC collected in 2010 and 2011 at $\sqrt{s} = 7$ TeV. They include searches in the $\mathrm{H} \to \mathrm{ZZ} \to 4\ell$ channel ($\ell = e, \mu$) by ATLAS [11] and CMS [12] and in the $\mathrm{H} \to \mathrm{ZZ} \to 2\ell 2\tau$ channel by CMS [13]. Search results combining these with various production and decay channels were reported by both collaborations. The results from CMS exclude the SM Higgs boson in the mass range 127–600 GeV at 95% confidence level (CL) [14].. ATLAS excludes 111.4–116.6 GeV, 119.4–122.1 GeV, and 129.2– 541 GeV at 95% CL [15, 16]. Direct searches for the SM Higgs boson at the LEP $\mathrm{e}^+\mathrm{e}^-$ collider and the Tevatron $\mathrm{p\bar{p}}$ collider have led, respectively, to a lower-mass bound of $m_{\mathrm{H}} > 114.4$ GeV [17], and to an exclusion in the range 162–166 GeV [18], at 95% CL. Indirect constraints from precision measurements favour the mass range $m_{\mathrm{H}} < 158$ GeV [19, 20] at 95% CL.

In this paper, a search in the four-lepton decay channels $\mathrm{H} \to 4\ell$ and $\mathrm{H} \to 2\ell 2\tau$, with $\ell =$ e or μ, is presented. The analysis is designed for a Higgs boson in the mass range $110 < m_{\mathrm{H}} < 600$ GeV. It re-uses the data collected at $\sqrt{s} = 7$ TeV by CMS in 2011, corresponding to an integrated luminosity of 5.05 fb^{-1}, combined with new data collected in 2012 at $\sqrt{s} = 8$ TeV, corresponding to an additional 5.26 fb^{-1}.

The search relies critically on the reconstruction, identification, and isolation of leptons. Compared to the previous CMS analyses, it profits from improved lepton reconstruction and isolation efficiencies, combined with the use of a discriminant exploiting the production and decay kinematics expected for the signal events. The analysis achieves high lepton reconstruction efficiencies for a ZZ system composed of two pairs of same-flavour and opposite-charge isolated leptons, $\mathrm{e}^+\mathrm{e}^-$, $\mu^+\mu^-$, or $\tau^+\tau^-$, in the measurement range $m_{4\ell}, m_{2\ell 2\tau} > 100$ GeV. One or both of the Z bosons can be off-shell. The single-resonant four-lepton production ($\mathrm{Z} \to 4\ell$) is used as a standard candle in the mass range $70 < m_{4\ell} < 100$ GeV [21]. The background sources include an irreducible four-lepton contribution from direct ZZ (or $\mathrm{Z}\gamma^*$) production via $\mathrm{q\bar{q}}$ annihilation and gg fusion. Reducible contributions arise from $\mathrm{Zb\bar{b}}$ and $\mathrm{t\bar{t}}$ where the final states contain two isolated leptons and two b jets producing secondary leptons. Additional background of instrumental nature arises from Z + jets and WZ + jets events where jets are misidentified as leptons.

2 CMS detector and experimental methods

Particles produced in the pp collisions are detected in the pseudorapidity range $|\eta| < 5$, where $\eta = -\ln[\tan(\theta/2)]$ and θ is the polar angle with respect to the direction of the proton beam. The CMS detector comprises a superconducting solenoid, providing a uniform magnetic field of 3.8 T in the bore, equipped with silicon pixel and strip tracking systems ($|\eta| < 2.5$) surrounded by a lead tungstate crystal electromagnetic calorimeter (ECAL) and a brass-scintillator hadronic calorimeter (HCAL) ($|\eta| < 3.0$). A steel/quartz-fiber Cherenkov calorimeter extends the coverage ($|\eta| < 5$). The steel return yoke outside the solenoid is instrumented with gas

ionization detectors used to identify muons ($|\eta| < 2.4$). A detailed description of the detector is given in Ref. [22].

A complete reconstruction of the individual particles emerging from each collision event is obtained via a particle-flow (PF) technique. This uses the information from all CMS sub-detectors to identify and reconstruct individual particles in the collision event [23, 24], with particles classified into mutually exclusive categories: charged hadrons, neutral hadrons, photons, muons, and electrons. For electrons, the basic collection of reconstructed candidates is first obtained separately. The electrons are reconstructed within the geometrical acceptance, $|\eta^{\mathrm{e}}| < 2.5$, and for $p_{\mathrm{T}}^{\mathrm{e}} > 7\,\mathrm{GeV}$. The reconstruction combines the information from clusters of energy deposits in the ECAL and the trajectory in the inner tracker [25, 26]. The track-cluster matching is initiated either "outside-in" from energy cluster measurements, or "inside-out" from track reconstruction. Trajectories in the tracker volume are reconstructed using a dedicated modeling of the electron energy loss and fitted with a Gaussian sum filter. Electrons are identified among the reconstruction candidates and then used, together with the other PF particles, to obtain a consistent description of the event. Their identification relies on a multivariate technique that combines observables sensitive to the amount of bremsstrahlung along the electron trajectory, the geometrical and momentum matching between the electron trajectory and associated clusters, as well as shower-shape observables. The multivariate identification is trained using a Higgs boson Monte Carlo (MC) sample for the signal and a W + 1 jet data sample for background, and the working point is optimized using a Z + 1 jet data sample. Muons are reconstructed within $|\eta^{\mu}| < 2.4$ and for $p_{\mathrm{T}}^{\mu} > 5\,\mathrm{GeV}$. The reconstruction combines the information from both the silicon tracker and the muon spectrometer. The matching between the inner and outer tracks is initiated either "outside-in", starting from a track in the muon system, or "inside-out", starting from a track in the silicon tracker. The PF muons are selected among the reconstructed muon track candidates by applying minimal requirements on the track components in the muon system and taking into account a matching with small energy deposits in the calorimeters [27]. Tau leptons are identified in their leptonic decay mode denoted τ_ℓ, with an electron or muon as measurable decay product, and in the semileptonic one denoted τ_{h}, with hadrons in the decay products. The PF particles are used to reconstruct τ_{h} with the "hadron-plus-strip" (HPS) algorithm [28]. The HPS algorithm optimizes the reconstruction and identification of specific τ_{h} decay modes. The π^0 components of the τ_{h} are first reconstructed and then combined with charged hadrons to reconstruct the τ_{h} decay modes. The neutrinos produced in all τ decays escape detection and are ignored in the reconstruction. The taus in this analysis are required to have $|\eta^{\tau_{\mathrm{h}}}| < 2.3$ and $p_{\mathrm{T}}^{\tau_{\mathrm{h}}} > 20\,\mathrm{GeV}$.

The isolation of individual e or μ leptons is measured relative to their transverse momentum p_{T}^{ℓ}, by summing over charged and neutral particles in a cone $\Delta R = \sqrt{(\eta^{\ell} - \eta^{i})^2 + (\phi^{\ell} - \phi^{i})^2} < 0.4$ around the lepton direction at the interaction vertex:

$$R_{\mathrm{Iso}}^{\ell} \equiv \left(\sum p_{\mathrm{T}}^{\mathrm{charged}} + \mathrm{MAX}\left[0, \sum E_{\mathrm{T}}^{\mathrm{neutral}} + \sum {E_{\mathrm{T}}}^{\gamma} - \rho \times A_{\mathrm{eff}}, \right] \right) / p_{\mathrm{T}}^{\ell} \ .$$

The $\sum p_{\mathrm{T}}^{\mathrm{charged}}$ is the scalar sum of the transverse momenta of charged hadrons originating from the primary vertex. The primary vertex is chosen as the vertex with the highest sum of p_{T}^2 of its constituent tracks. The $\sum E_{\mathrm{T}}^{\mathrm{neutral}}$ and $\sum {E_{\mathrm{T}}}^{\gamma}$ are the scalar sums of the transverse energies for neutral hadrons and photons, respectively. The latter excludes photons that are candidates for final-state radiation (FSR) from the lepton (see below). The term $\rho \times A_{\mathrm{eff}}$ subtracts an estimate obtained using a "jet area" technique [29] of the transverse energy from neutrals in the isolation cone coming from pileup of additional pp collisions. The transverse energy density ρ is calculated in each event as the median of the neutral-energy distribution around "jets" (any

PF jet in the event having $p_T^{jet} > 3$ GeV) with mean effective $\eta - \phi$ area A_{eff}. A small residual dependence on the number of pileup collisions is absorbed as a correction factor on A_{eff}. The electrons or muons are considered isolated in the $H \to 4\ell$ analysis if $R_{Iso}^{\ell} < 0.4$. Tighter isolation requirements are imposed for leptons in the $H \to 2\ell 2\tau$ analysis depending on the assignment to either the $Z \to \ell^+\ell^-$, for which $R_{Iso}^{\ell} < 0.25$ is required, or to $Z \to \tau_\ell + \tau_h$, for which $R_{Iso}^{\ell} < 0.1$ is required.

The electron or muon pairs from Z decays should originate from the primary vertex. This is ensured by requiring that the significance of the impact parameter to the event vertex, SIP_{3D}, satisfies $|SIP_{3D} = \frac{IP}{\sigma_{IP}}| < 4$ for each lepton. The IP is the lepton impact parameter in three dimensions at the point of closest approach with respect to the primary interaction vertex, and σ_{IP} the associated uncertainty.

The efficiencies for the product of reconstruction, identification, and isolation of primary e or μ leptons are measured in data, using a tag-and-probe technique [30] based on an inclusive sample of Z events. The measurements are performed in several bins of p_T^{ℓ} and $|\eta|$. The efficiencies for selecting electrons in the ECAL barrel (endcaps) varies from about 71% (65%) for $7 < p_T^e < 10\,\text{GeV}$ to 82% (73%) at $p_T^e \simeq 10\,\text{GeV}$, and reaches 90% (89%) for $p_T^e \simeq 20\,\text{GeV}$. It drops to about 85% in the transition region, $1.44 < |\eta| < 1.57$, between the ECAL barrel and endcaps. The muons are reconstructed and identified with efficiencies above ~98% in the full $|\eta^\mu| < 2.4$ range. The performance for the tau lepton identification is discussed in Ref. [28].

Photons reconstructed within $|\eta^\gamma| < 2.4$ are possible FSR candidates. To be accepted as FSR, a reconstructed photon must either have $p_T^\gamma > 2\,\text{GeV}$ and be found within a conical distance $\Delta R < 0.07$ from a selected lepton candidate, or have $p_T^\gamma > 4\,\text{GeV}$ and be found isolated within the conical distance of $0.07 < \Delta R < 0.5$ around a selected lepton candidate. The photon isolation observable R_{Iso}^γ is obtained by summing over the transverse momenta of charged hadrons, other photons and neutral hadrons identified by the PF reconstruction in a cone of size $\Delta R = 0.3$ around the candidate photon direction, correcting for pileup, and dividing by the photon transverse momentum, p_T^γ. Isolated photons must satisfy $R_{Iso}^\gamma < 1$.

The performance of the FSR selection algorithm has been measured using MC simulation samples, and the rate was verified with single-Z data events. The photons within the acceptance for the FSR selection are measured with an efficiency of $\simeq$ 50% and with a mean purity of 80%. FSR photons are selected in 5% of single-Z events with muon pairs, and 0.5% of single-Z events with electron pairs. A gain of $\simeq$ 3% (2%, 1%) in efficiency is expected for the selection of $H \to 4\mu$ (2e2μ, 4e) events in this analysis.

3 Datasets

Collision events are selected by the trigger system that requires the presence of a pair of electrons or a pair of muons. A cross-trigger requiring an electron and a muon is also used for the 2012 data. The requirements on the transverse energy (transverse momenta) for the first and second lepton are 17 and 8 GeV respectively. The trigger efficiency within the acceptance of this analysis is greater than 99% (96%, 98%) in the 4μ (4e , 2e2μ) channels, for a Higgs boson signal with $m_H > 120\,\text{GeV}$, and in the $2\ell 2\tau$ channels at high mass, for a Higgs boson signal with $m_H > 180\,\text{GeV}$.

Monte Carlo (MC) samples for the SM Higgs boson signal and for background processes are used to optimize the event selection and to evaluate the acceptance and systematic uncertainties. The Higgs boson signals from gluon-fusion ($gg \to H$), and vector-boson fusion ($qq \to$

qqH), are generated with POWHEG [31] at next-to-leading order (NLO) and a dedicated generator from Ref. [32] for angular correlations. Additional samples of WH, ZH, and $t\bar{t}H$ events are generated with PYTHIA [33]. Events at generator level are reweighted according to the total cross section $\sigma(pp \to H)$, which contains contributions from gluon fusion up to next-to-next-to-leading order (NNLO) and next-to-next-to-leading log taken from Refs. [34–45] and from the weak-boson fusion contribution computed at NNLO in Refs. [37, 46–50]. The total cross section is scaled by the branching fraction $\mathcal{B}(H \to 4\ell)$ calculated with PROPHECY4F, which includes NLO QCD and electroweak corrections and all interference effects at NLO [37, 51–54], in particular effects specific to the 4e and 4μ channels. The SM background contribution from ZZ production via $q\bar{q}$ is generated at NLO with POWHEG, while other diboson processes (WW, WZ) are generated with MADGRAPH [55] with cross sections rescaled to NLO predictions. The $gg \to ZZ$ contribution is generated with GG2ZZ [56]. The $Zb\bar{b}$, $Zc\bar{c}$, $Z\gamma$, and $Z +$ light jets samples are generated with MADGRAPH, as contributions to inclusive Z production, with cross sections rescaled to NNLO prediction for inclusive Z production. The $t\bar{t}$ events are generated at NLO with POWHEG. The generation takes into account the internal initial-state and final-state radiation effects which can lead to the presence of additional hard photons in an event. For leading-order generators, the default set of parton distribution functions (PDF) used to produce these samples is CTEQ6L [57], while CT10 [58] is used for NLO generators. All generated samples are interfaced with PYTHIA. All events are processed through a detailed simulation of the CMS detector based on GEANT4 [59] and are reconstructed with the same algorithms that are used for data.

4 Event selection and kinematics

The event selection is built to give a mutually exclusive set of signal candidates in the $H \to 4\ell$ and $H \to 2\ell 2\tau$ channels.

The signal candidates in the 4ℓ analysis are first selected. The selection uses well identified and isolated primary leptons. The lepton isolation requirements suppress the Z+jet, $Zb\bar{b}$ and $t\bar{t}$ backgrounds. The requirement on the significance of the impact parameter to the event vertex $|\mathrm{SIP}_{3D}| < 4$ further suppresses the $Zb\bar{b}$ and $t\bar{t}$ backgrounds. When building the Z candidates, only the FSR photons associated with the closest lepton and which make the "dressed" lepton-pair mass closer to the nominal Z mass are kept, with a maximum mass $m_{\ell\ell\gamma} < 100\,\mathrm{GeV}$. We require a Z candidate formed with a pair of leptons of the same flavour and opposite charge ($\ell^+\ell^-$). The pair with an invariant mass closest to the nominal Z mass is denoted m_{Z_1} and retained if it satisfies $40 < m_{Z_1} < 120\,\mathrm{GeV}$. We then consider all remaining leptons and require a second pair of $\ell^+\ell^-$, with mass denoted m_{Z_2}, to satisfy $12 < m_{Z_2} < 120\,\mathrm{GeV}$. The 12 GeV cut provides an optimal sensitivity for a Higgs boson mass hypothesis in the range $110 < m_H < 160\,\mathrm{GeV}$. If more than one Z_2 candidate satisfies all criteria, the ambiguity is resolved by choosing the leptons of highest p_T. Among the four selected leptons forming Z_1 and the Z_2, at least one should have $p_T > 20\,\mathrm{GeV}$ and another one have $p_T > 10\,\mathrm{GeV}$. These p_T thresholds ensure that the selected events have leptons on the high-efficiency plateau for the trigger. To further protect against leptons originating from hadron decays in jet fragmentation or from the decay of low-mass hadronic resonances, we require that any opposite-charge pair of leptons chosen among the four selected leptons (irrespective of flavour) satisfy $m_{\ell\ell'} > 4\,\mathrm{GeV}$. The phase space for the search of the SM Higgs boson is defined by restricting the mass range to $m_{4\ell} > 100$ GeV. A higher minimal threshold on m_{Z_1} and m_{Z_2} could be used for higher m_H values but only with marginal improvement of the sensitivity. For comparison we define a "high-mass" selection by requiring $m_{Z_1}, m_{Z_2} > 60\,\mathrm{GeV}$.

For the search in the $2\ell2\tau$ final state, events are required to have one $Z_1 \to \ell^+\ell^-$ candidate with one lepton at $p_T > 20\,\text{GeV}$ and the other at $p_T > 10\,\text{GeV}$, and a $Z_2 \to \tau^+\tau^-$, with τ decaying into μ, e or τ_h. The leptons from the τ leptonic decays are required to have $p_T^\ell > 10\,\text{GeV}$. The τ_h are required to have $p_T^{\tau_h} > 20\,\text{GeV}$. The invariant mass of the reconstructed Z_1 is required to satisfy $60 < m_{\ell\ell} < 120\,\text{GeV}$, and that of the Z_2 to satisfy $m_{\tau\tau} < 90\,\text{GeV}$. Thus, the $2\ell2\tau$ final states contribute only to the "high-mass" selection.

The event yields are found to be in good agreement with the MC background expectation at each step of event selection.

Kinematics of the Higgs or exotic boson decay to ZZ final state has been extensively studied in the literature [32, 60–70]. Since the Higgs boson is spinless, the angular distribution of its decay products is independent of the production mechanism. Five angles $(\theta^*, \Phi_1, \theta_1, \theta_2, \Phi)$ defined in Ref. [32] and the invariant masses of the lepton pairs, m_{Z_1} and m_{Z_2}, fully describe the kinematics of the $H \to ZZ \to 4\ell$ process at a given mass of the four-lepton system in their centre-of-mass frame. These observables provide significant discriminating power between signal and background.

We use a matrix element likelihood analysis (MELA). We construct a kinematic discriminant (KD) based on the probability ratio of the signal and background hypotheses, MELA KD $= \mathcal{P}_{\text{sig}}/(\mathcal{P}_{\text{sig}} + \mathcal{P}_{\text{bkg}})$, as described in Ref. [32]. The likelihood ratio is defined for each value of $m_{4\ell}$. The signal and $q\bar{q} \to ZZ$ background analytical parametrisations are taken from Refs. [32] and [70], respectively, and include the phase-space and Z propagator terms. When $m_{4\ell}$ is above the $2m_Z$ threshold, the two Z bosons are on-shell and no separation is provided by m_{Z_1} and m_{Z_2}, therefore leaving only the five angles in the parametrisation. When $m_{4\ell}$ is below the $2m_Z$ threshold, background has significant contribution from the $q\bar{q} \to ZZ^{(*)}/Z\gamma^{(*)}$ processes and instead of analytical parametrisation it is tabulated in a correlated template distribution using POWHEG simulation at generator level.

5 Background control and systematics

We rely on MC simulation to evaluate the local density ($\Delta N/\Delta m_{4\ell}$) of events expected as a function of the mass $m_{4\ell}$ from the ZZ background. Following the prescription used in the previous analysis, the cross section for ZZ production at NLO is calculated with MCFM [71–73]. This includes the dominant process of $q\bar{q}$ annihilation, as well as gluon fusion. The theoretical uncertainties are computed as a function of $m_{4\ell}$, varying both the QCD renormalisation and factorization scales and the PDF set, following the PDF4LHC recommendations [74–78]. The uncertainties for the QCD and PDF scales for each final state are on average 8%. The number of predicted $ZZ \to 4\ell$ events and their uncertainties after the signal selection are given in Table 1.

To estimate the reducible ($Zb\bar{b}$, $t\bar{t}$) and instrumental (Z + light jets, WZ + jets) backgrounds, a Z_1+X background control region, well separated from the signal region, is defined. In addition, a sample $Z_1 + \ell_{\text{reco}}$, with at least one reconstructed lepton object is defined for the measurement of the lepton misidentification probability — the probability for a reconstructed object to pass the isolation and identification requirements. The contamination from WZ in these events is suppressed by requiring the imbalance of the measured energy deposition in the transverse plane to be below 25 GeV. The lepton misidentification probability is compared, and found compatible, with the one derived from MC simulation. The event rates measured in the background control region are extrapolated to the signal region.

For the 4ℓ background estimate, two different approaches are used. Both start by relaxing the

isolation and identification criteria for two additional reconstructed lepton objects. A first approach follows from the previous CMS analysis. The additional pair of leptons is required to have the same charge (to avoid signal contamination) and same flavour ($e^{\pm}e^{\pm}, \mu^{\pm}\mu^{\pm}$), a reconstructed invariant mass $m_{Z_2} > 12\,\text{GeV}$, and $m_{4\ell} > 100\,\text{GeV}$. The expected number of Z+X background events in the signal region is obtained by taking into account the lepton misidentification probability for each of the two additional leptons. The second method uses the control region with two opposite-sign leptons failing the isolation and identification criteria, and using the misidentification probability to extrapolation to the signal region. In addition, a control region with three passing and one failing lepton is also used to account for contributions from backgrounds with three prompt leptons and one misidentified lepton. Comparable background counts in the signal region are found within uncertainties from both methods. An envelope comprising these results is used as the final estimate in Table 1.

Systematic uncertainties are evaluated from data for trigger (1.5%), and combined lepton reconstruction, identification and isolation efficiencies (varying from 1.2% in the 4μ channel at high masses to about 11% in $4e$ channel at low masses). The uncertainty associated with τ_h identification and isolation is 6%. Uncertainties on τ_h energy scale (3%) contribute to variation in the shape of the mass spectrum. Systematic uncertainties on energy-momentum calibration (0.4% for muons and 0.2% for electrons), and energy resolution are accounted for by their effects on the reconstructed mass distributions. The effect of the energy resolution uncertainties is taken into account by introducing a 20% uncertainty on the simulated width of the signal mass peak. To validate the level of accuracy with which the absolute mass scale and resolution are known, we use $Z \to \ell\ell$ and $J/\psi \to \ell\ell$ events. Additional systematic uncertainties arise from limited statistical precision in the reducible background control regions. All reducible and instrumental background sources are derived from control regions, and the comparison of data with the background expectation in the signal region is independent of the uncertainty on the LHC integrated luminosity of the data sample. This uncertainty (4.4%) [79] enters the evaluation of the ZZ background and in the calculation of the cross section limit through the normalisation of the signal. Systematic uncertainties on the Higgs boson cross section (17 – 20%) and branching fraction (2%) are taken from Ref. [37].

6 Results

The reconstructed four-lepton invariant-mass distributions for the 4ℓ, combining the 4e, 4μ, and $2e2\mu$ channels, are shown in Fig. 1 (left) and compared with the expectation from SM background processes. The measurements are globally well described by the background. The peak of the $Z \to 4\ell$ standard candle around $m_{4\ell} = m_Z$ is observed as expected. The measured distribution at higher mass is in agreement with the expectation dominated by the irreducible ZZ background. The reconstructed visible mass distributions for the $2\ell2\tau$ selection, combining all the $\ell^+\ell^-\tau^+\tau^-$ final states, are shown in Fig. 1 (right) and compared to SM background expectation. The background shapes are taken from MC simulation and the rates are normalised to the values obtained using a method based on data. The measured distribution is well described by the SM background expectation.

The number of candidates observed as well as the estimated background in the signal region are reported in Table 1, for the selection in the full mass measurement range for the Higgs boson search, $100 < m_{4\ell}, m_{2\ell2\tau} < 800\,\text{GeV}$. The expected number of signal events is also given for several Higgs boson mass hypotheses. The observed event rates for the various channels are compatible with SM background expectation.

The distributions of the MELA KD versus the four-lepton reconstructed mass $m_{4\ell}$ is shown for

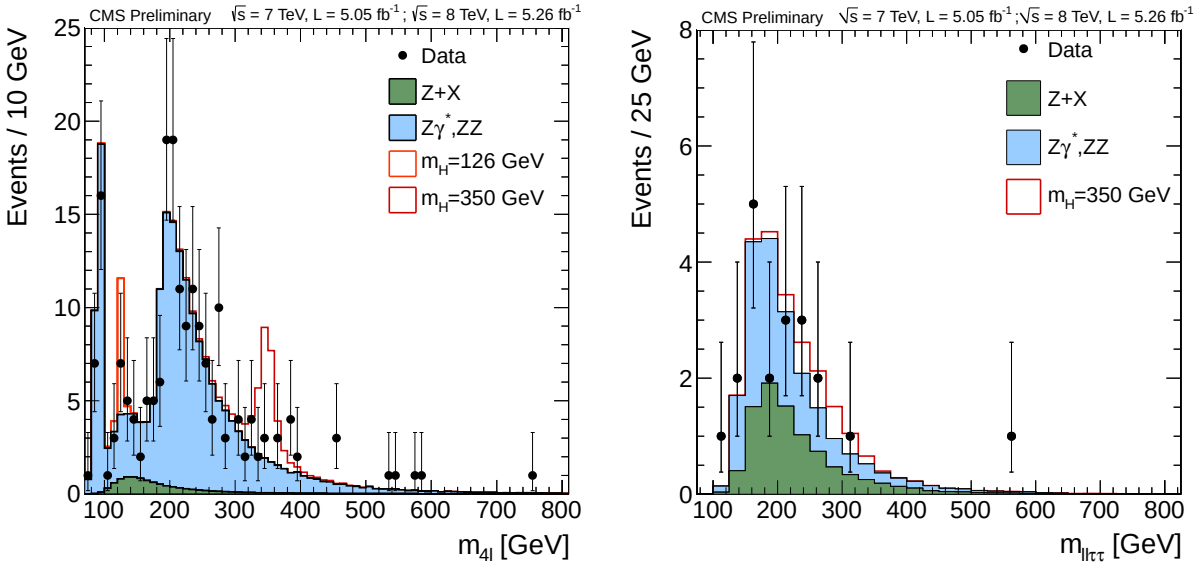

Figure 1: Distribution of the four-lepton reconstructed mass in full mass range for the sum of the 4e, 4μ, and 2e2μ channels (left), and for the sum over all $\ell^+\ell^-\tau^+\tau^-$ channels (right). Points represent the data, shaded histograms represent the background and unshaded histogram the signal expectations. The distributions are presented as stacked histograms. The measurements are presented for the sum of the data collected at $\sqrt{s} = 7$ TeV and $\sqrt{s} = 8$ TeV.

the selected events and compared to SM background expectation in Fig. 2. The distribution of events in the $(m_{4\ell}, \mathrm{KD})$ plane is seen to agree well with the SM expectation in the high mass range (Fig. 2, right). Considering high values of the MELA KD > 0.5, three events are observed in the range $520 < m_{4\ell} < 600$ GeV and a clustering of events is apparent in the low mass range (Fig. 2, left).

The measured distributions are compared with the expectation from SM background processes, and exclusion limits at 95% CL on the ratio of the production cross section for the Higgs boson to the SM expectation are derived. For this, the $(m_{4\ell}, \mathrm{KD})$ distributions of the selected events are split into six categories based on three final states and two running periods (7 and 8 TeV). These events are examined for 183 hypothetical Higgs boson masses in a range between

Table 1: The number of event candidates observed, compared to the mean expected background and signal rates for each final state. For the ZX background, the estimations are based on data. The results are given integrated over the full mass measurement range for the Higgs boson search from 100 to 800 GeV.

Channel	4e	4μ	2e2μ	4ℓ	$2\ell2\tau$
ZZ background	29.3 ± 3.4	49.0 ± 5.1	75.5 ± 8.0	153.7 ± 10.1	12.1 ± 1.5
Z+X	$3.0^{+2.7}_{-1.9}$	$2.2^{+1.6}_{-1.3}$	$5.0^{+4.0}_{-3.0}$	$10.2^{+5.0}_{-3.8}$	8.9 ± 2.5
All backgrounds	$32.3^{+4.4}_{-3.9}$	$51.2^{+5.3}_{-5.3}$	$80.5^{+9.0}_{-8.6}$	$163.9^{+11.3}_{-10.8}$	21.0 ± 2.9
$m_H = 200$ GeV	8.3 ± 2.0	13.3 ± 2.7	21.6 ± 4.5	43.2 ± 5.6	2.9 ± 0.7
$m_H = 350$ GeV	4.8 ± 1.2	7.5 ± 1.6	12.7 ± 2.9	24.9 ± 3.5	3.1 ± 0.8
$m_H = 500$ GeV	1.7 ± 0.8	2.6 ± 1.2	4.4 ± 2.0	8.7 ± 2.4	1.4 ± 0.7
Observed	32	47	93	172	20

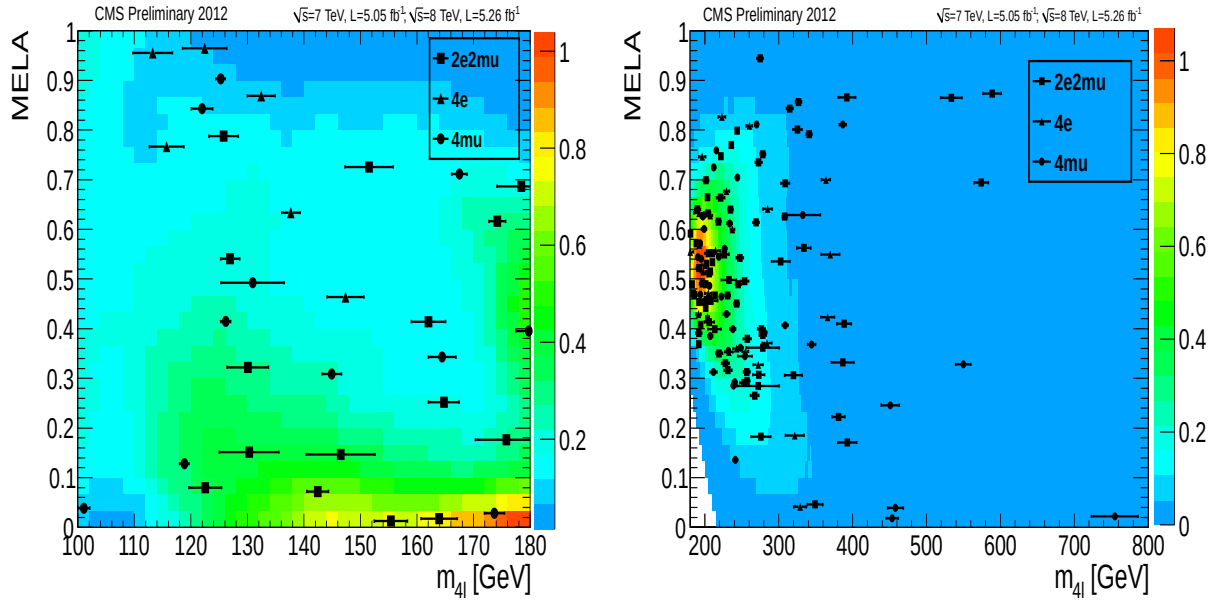

Figure 2: Distribution of the MELA KD versus the four-lepton reconstructed mass $m_{4\ell}$ in the low-mass (left) and full-mass (right) regions. The points representing the individual events are shown together with their reconstructed mass uncertainties. The contours represent the expected relative density of background events. The points show data with measured invariant mass uncertainties.

110 GeV and 600 GeV, where the mass steps are optimized to account for the expected width, Γ_{H}, and resolution for the measurement of m_{H} [80]. For each mass hypothesis, we perform a simultaneous likelihood fit of the six two-dimensional $(m_{4\ell}, \mathrm{KD})$ distributions using the statistical approaches discussed in Ref. [80]. As a cross-check, we have also studied one-dimensional $m_{4\ell}$ distributions and found consistent, but systematically higher expected limits. We adopt the modified frequentist construction $\mathrm{CL_s}$ [80–82] as the primary method for reporting limits. As a complementary method to the frequentist paradigm, we use the Bayesian approach [83] and find consistent results.

The probability distribution of $\mathcal{P}(m_{4\ell})$ for the background is parametrised with empirical functions using MC simulation for ZZ background and data control regions for $\mathrm{Z}+\mathrm{X}$ background. The reconstructed signal $m_{4\ell}$ distributions are described with a relativistic Breit-Wigner parametrization convoluted with a Crystal-Ball function [84]. The correlated two-dimensional $(m_{4\ell}, \mathrm{KD})$ distribution is described by the one-dimensional probability distribution $\mathcal{P}(m_{4\ell})$ multiplied by a two-dimensional template distribution normalised in the KD dimension. This template distribution is obtained from simulation for both signal and ZZ background, accounting for interference effects of identical leptons in the final state. It has been verified that the KD distribution of the $\mathrm{Z}+\mathrm{X}$ background is consistent with that of the ZZ background, and any potential small difference is accounted for in the systematic uncertainties.

For the $2\ell 2\tau$ channels, signal and background shape templates are taken from simulation, with the background yields normalised to the data-driven yields described above. Shape variations due to τ energy scale uncertainties are accounted for by vertical template morphing. Due to the limited number of simulated events, the reducible background shape was taken with relaxed isolation requirements on the second Z boson. Normalizations for backgrounds vary within

the uncertainties. All systematic uncertainties are included in the likelihood with log-normal distributions.

The upper limits obtained from the combination of the 4ℓ and $2\ell 2\tau$ channels are shown in Fig. 3 (left). The SM Higgs boson is excluded by the four-lepton channels at 95% CL in the range 131–525 GeV, except for the small range 162–172 GeV where the branching ratio for the $H \to ZZ$ decay is disfavoured. The upper limits in the low-mass region are given in Fig. 4. The local

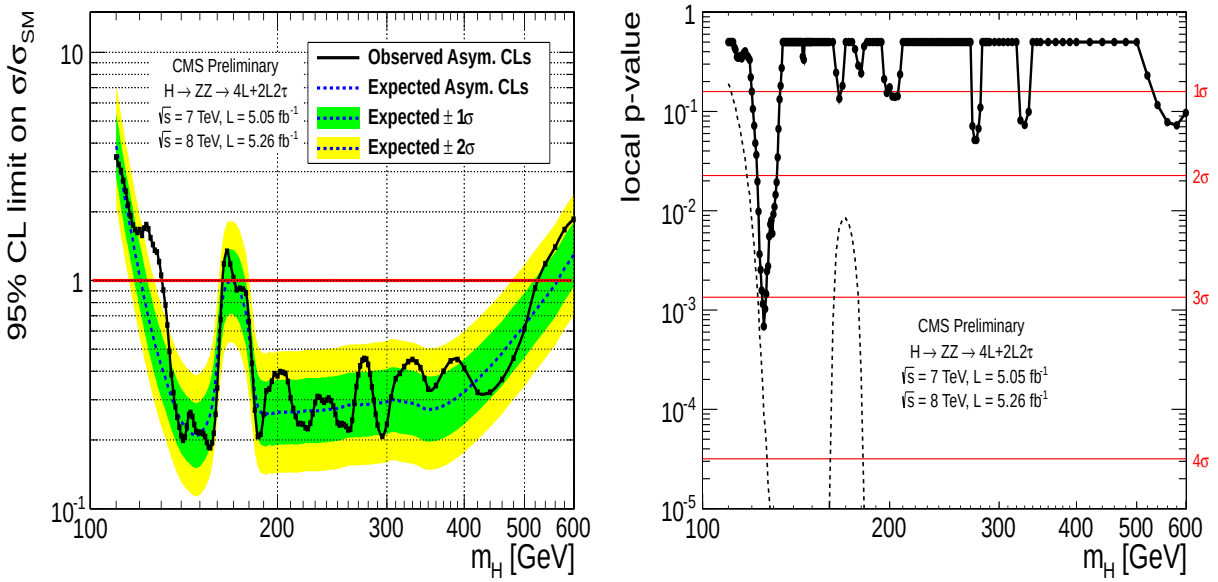

Figure 3: Observed and expected 95% CL upper limit (left) on the ratio of the production cross section to the SM expectation. The 68% and 95% ranges of expectation for the background-only model are also shown with green and yellow bands, respectively. Significance of the local excess (right) with respect to the standard model background expectation as a function of the Higgs boson mass in the full interpretation mass range 110-600 GeV.

p-values, representing the significance of local excesses relative to the background expectation, are shown for the full mass range as a function of m_{H} in Fig. 3 (right). The minimum of the local p-value is reached at low mass around $m_{4\ell} = 125.5$ GeV. The anatomy of the most significant excess with respect to the SM background expectation is discussed in more details below.

An excess of events is observed in the low mass range in the 4ℓ channel. The number of candidates observed as well as the estimated background in the signal region are reported in Table 2, for the selection in the low mass range. A relatively flat background is expected in this mass range.

The distribution of the four-lepton reconstructed mass for the sum of the 4e, 4μ, and $2e2\mu$ channels, and the distribution of the MELA KD versus the four-lepton reconstructed mass $m_{4\ell}$ are shown in Fig. 5 in the low mass range. A signal-like clustering of events is apparent at high values of KD and for $m_{\mathrm{H}} \approx 125$ GeV. As an illustration, the reconstructed four-lepton invariant-mass distributions for the 4ℓ are shown in Fig. 6 for a $m_{4\ell}$ slice and for events with KD > 0.5. A clustering of events is clearly visible near $m_{4\ell} \approx 125.5$ GeV.

The local p-values in the low mass region are shown in Fig. 7. The minimum of the local p-value is reached for the Higgs boson mass hypothesis of 125.5 GeV and corresponds to a local significance of 3.2σ. The local significance of 2.2σ is reached in the 1D fit without the MELA

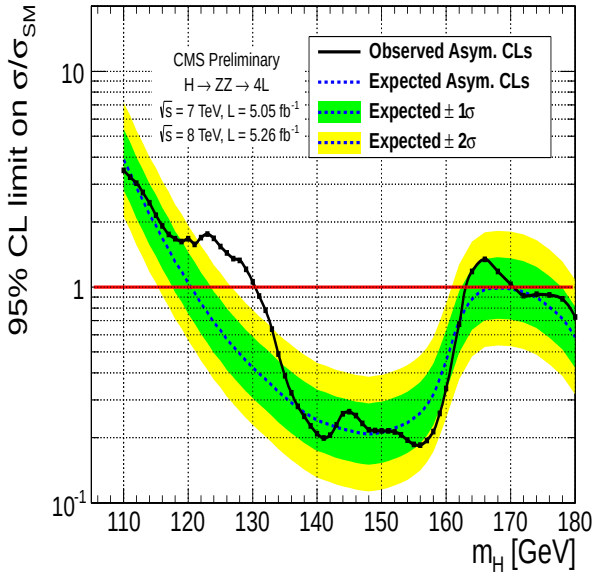

Figure 4: Observed and expected 95% CL upper limit on the ratio of the production cross section to the SM expectation, in the low-mass region. The 68% and 95% ranges of expectation for the background-only model are also shown with green and yellow bands, respectively.

KD. The average expected significance for a standard model Higgs boson at this mass is 3.8σ and 3.2σ for the 2D and 1D fits, respectively.

To extract from the 4ℓ measurements a signal strength modifier μ for a SM Higgs boson signal ($\mu \times \sigma_{\rm SM}$) and a most probable mass, we perform a likelihood scan on data in the 2D space of $m_{\rm H}$ vs. μ. At each point (m_H, μ), the likelihood is minimized with respect to all nuisance parameters. The global minimum is located at $m_H = 125.6$ GeV and $\mu = 0.7$.

Using simulation it was found that the MELA KD distribution for signal at mass around $m_H = 125$ GeV is similar for a scalar, pseudo-scalar, or a spin-two resonance with the minimal couplings [32]. Therefore the analysis presented is nearly model-indepedent in the low mass region. We also studied the discrimination between the pseudo-scalar and scalar hypotheses using a modified MELA discriminant, with the pseudo-scalar signal hypothesis probability used in place of background probability. The expected separation between the two hypotheses

Table 2: The number of event candidates observed, compared to the mean expected background and signal rates for each final state. For the Z +X background, the estimations are based on data. The results are given integrated the mass range from 110 to 160 GeV.

Channel	4e	4μ	2e2μ	4ℓ
ZZ background	2.7 ± 0.3	5.7 ± 0.6	7.2 ± 0.8	15.5 ± 1.0
Z+X	$1.2^{+1.1}_{-0.8}$	$0.9^{+0.7}_{-0.6}$	$2.3^{+1.8}_{-1.4}$	$4.4^{+2.2}_{-1.7}$
All backgrounds	$3.9^{+1.1}_{-0.8}$	$6.6^{+0.9}_{-0.8}$	$9.5^{+2.0}_{-1.6}$	$19.9^{+2.4}_{-2.0}$
$m_{\rm H} = 120$ GeV	0.8 ± 0.2	1.6 ± 0.3	1.9 ± 0.5	4.4 ± 0.6
$m_{\rm H} = 126$ GeV	1.5 ± 0.5	3.0 ± 0.6	3.8 ± 0.9	8.3 ± 1.2
$m_{\rm H} = 130$ GeV	2.1 ± 0.7	4.1 ± 0.8	5.4 ± 1.3	11.6 ± 1.6
Observed	6	6	9	21

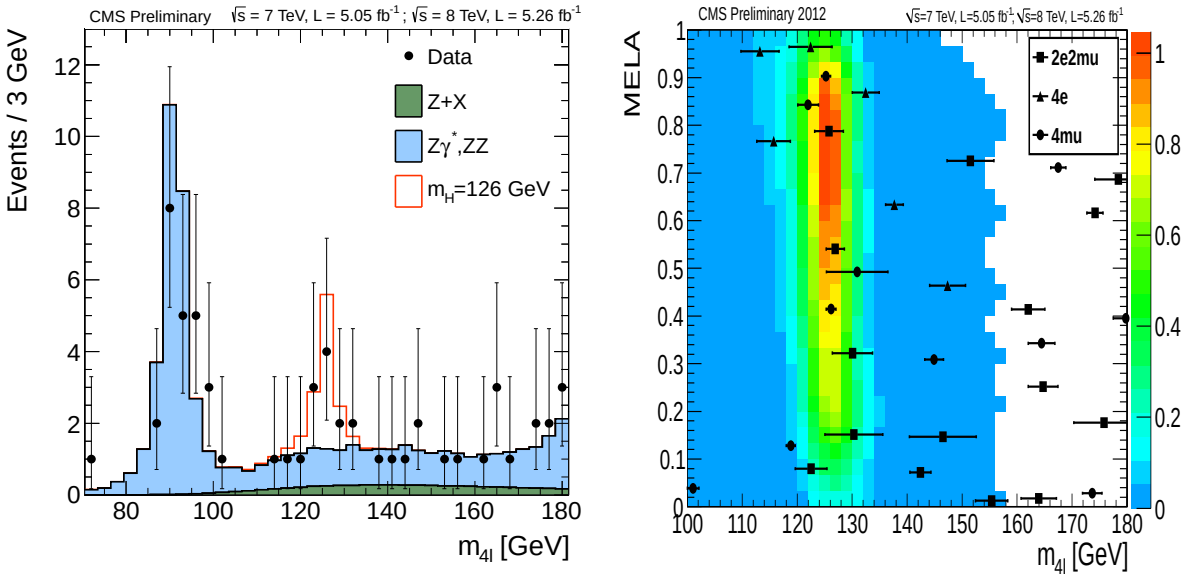

Figure 5: Distribution of the four-lepton reconstructed mass for the sum of the 4e, 4μ, and 2e2μ channels (left). Points represent the data, shaded histograms represent the background and unshaded histogram the signal expectations. Distribution of the MELA KD versus the four-lepton reconstructed mass $m_{4\ell}$ (right) with contours shown for expected relative density of signal events for hypothesis $m_H = 126$ GeV. The points show data with measured invariant mass uncertainties.

with the present data sample is 1.6 standard deviations and additional 25 fb^{-1} are needed to reach the 3σ expected separation.

7 Summary

In summary, a search for the standard model Higgs boson has been presented in the four-lepton decay modes, $\text{H} \to \text{ZZ} \to 4\ell$ and $\text{H} \to \text{ZZ} \to 2\ell 2\tau$. The mass distributions measured with four-lepton invariant masses $m_{4\ell}$ or $m_{2\ell 2\tau} > 100$ GeV are found to be globally consistent with the standard model background expectation. The measurements are interpreted by using for each event the information from the measured four-lepton mass and a kinematic discriminant. Upper limits at 95% confidence level exclude the standard model Higgs boson in the range 131–162 and 172–525 GeV, while the expected exclusion range is 121–570 GeV. An excess of events is observed in the mass range $120 < m_{4\ell} < 130$ GeV, making the observed limits weaker than expected in the absence of a signal. These events cluster around a mass $m_{4\ell} \simeq 125.5$ GeV, giving rise to a local excess with respect to the background expectation, with a significance of 3.2σ. This result constitutes evidence for a new massive state.

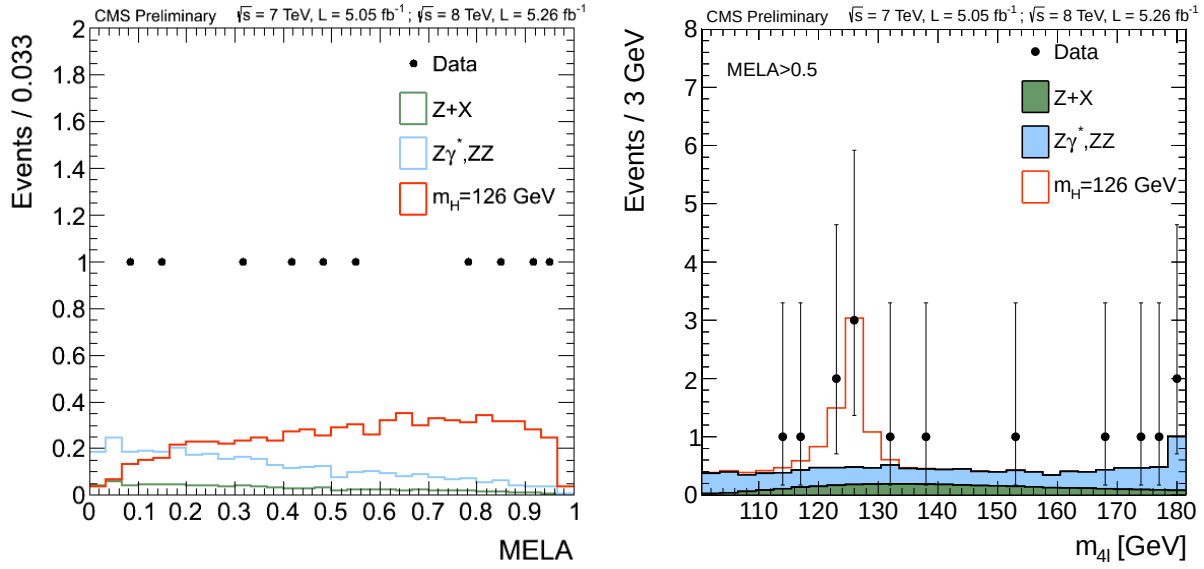

Figure 6: Distribution of the MELA kinematic discriminant for events in the mass region $121 < m_{4\ell} < 131\,\text{GeV}$ (left). Distribution of the four-lepton reconstructed mass for the sum of the 4e, 4μ, and 2e2μ channels for events with a value KD > 0.5 of the MELA kinematic discriminant. Points represent the data, shaded histograms represent the background and unshaded histogram the signal expectations. The measurements are presented for the sum of the data collected at $\sqrt{s} = 7\,\text{TeV}$ and $\sqrt{s} = 8\,\text{TeV}$.

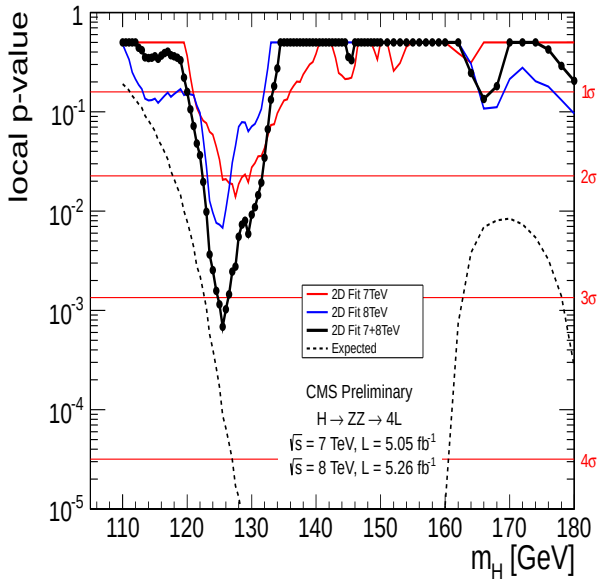

Figure 7: Significance of the local excess with respect to the standard model background expectation as a function of the Higgs boson mass. The results are shown for the full data sample and for $\sqrt{s} = 7$ and 8 TeV samples separately in the low-mass region only.

References

[1] S. L. Glashow, "Partial Symmetries of Weak Interactions", *Nucl. Phys.* **22** (1961) 579, doi:10.1016/0029-5582(61)90469-2.

[2] S. Weinberg, "A Model of Leptons", *Phys. Rev. Lett.* **19** (1967) 1264, doi:10.1103/PhysRevLett.19.1264.

[3] A. Salam, "Weak and electromagnetic interactions", in *Elementary particle physics: relativistic groups and analyticity*, N. Svartholm, ed., p. 367. Almquvist & Wiskell, 1968. Proceedings of the eighth Nobel symposium.

[4] F. Englert and R. Brout, "Broken Symmetry and the Mass of Gauge Vector Mesons", *Phys. Rev. Lett.* **13** (1964) 321, doi:10.1103/PhysRevLett.13.321.

[5] P. W. Higgs, "Broken symmetries, massless particles and gauge fields", *Phys. Lett.* **12** (1964) 132, doi:10.1016/0031-9163(64)91136-9.

[6] P. W. Higgs, "Broken Symmetries and the Masses of Gauge Bosons", *Phys. Rev. Lett.* **13** (1964) 508, doi:10.1103/PhysRevLett.13.508.

[7] G. S. Guralnik, C. R. Hagen, and T. W. B. Kibble, "Global Conservation Laws and Massless Particles", *Phys. Rev. Lett.* **13** (1964) 585, doi:10.1103/PhysRevLett.13.585.

[8] P. W. Higgs, "Spontaneous Symmetry Breakdown without Massless Bosons", *Phys. Rev.* **145** (1966) 1156, doi:10.1103/PhysRev.145.1156.

[9] T. W. B. Kibble, "Symmetry breaking in non-Abelian gauge theories", *Phys. Rev.* **155** (1967) 1554, doi:10.1103/PhysRev.155.1554.

[10] L. Evans and P. Bryant, "LHC Machine", *JINST* **3** (2008) S08001, doi:10.1088/1748-0221/3/08/S08001.

[11] ATLAS Collaboration, "Search for the Standard Model Higgs boson in the decay channel $H \to ZZ^{(*)} \to 4l$ with 4.8 fb^{-1} of pp collision data at $\sqrt{s} = 7$ TeV with ATLAS", *Phys. Lett.* **B710** (2012) 383–402, arXiv:1202.1415.

[12] CMS Collaboration, "Search for the standard model Higgs boson in the decay channel H to ZZ to 4 leptons in pp collisions at $\sqrt{s} = 7$ TeV", arXiv:1202.1997.

[13] CMS Collaboration, "Search for the standard model Higgs boson in the H to ZZ to ll to $\tau\tau$ decay channel in pp collisions at $\sqrt{s} = 7$ TeV", *JHEP* **1203** (2012) 081, arXiv:1202.3617.

[14] CMS Collaboration, "Combined results of searches for the standard model Higgs boson in pp collisions at $\sqrt{s} = 7$ TeV", *Phys. Lett.* **B710** (2012) 26–48, arXiv:1202.1488.

[15] ATLAS Collaboration, "Combined search for the Standard Model Higgs boson using up to 4.9 fb^{-1} of pp collision data at $\sqrt{s} = 7$ TeV with the ATLAS detector at the LHC", *Phys. Lett.* **B710** (2012) 49–66, arXiv:1202.1408.

[16] ATLAS Collaboration, "Combined search for the Standard Model Higgs boson in pp collisions at sqrt(s) = 7 TeV with the ATLAS detector", arXiv:1207.0319. Submitted to *Phys. Rev. D*.

[17] ALEPH, DELPHI, L3, OPAL Collaborations, and the LEP Working Group for Higgs boson searches, "Search for the standard model Higgs boson at LEP", *Phys. Lett. B* **565** (2003) 61, doi:10.1016/S0370-2693(03)00614-2, arXiv:hep-ex/0306033.

[18] CDF and D0 Collaborations, "Combination of Tevatron Searches for the Standard Model Higgs Boson in the W^+W^- Decay Mode", *Phys. Rev. Lett.* **104** (2010) 061802, doi:10.1103/PhysRevLett.104.061802.

[19] ALEPH, CDF, D0, DELPHI, L3, OPAL, SLD Collaborations, the LEP Electroweak Working Group, the Tevatron Electroweak Working Group, and the SLD Electroweak and Heavy Flavour Groups, "Precision Electroweak Measurements and Constraints on the Standard Model", technical report, (2010).

[20] ALEPH, CDF, D0, DELPHI, L3, OPAL, SLD Collaborations, the LEP Electroweak Working Group, the Tevatron Electroweak Working Group, and the SLD Electroweak and Heavy Flavour Groups, "Precision electroweak measurements on the Z resonance", *Phys. Rept.* **427** (2006) 257, doi:10.1016/j.physrep.2005.12.006, arXiv:hep-ex/0509008.

[21] CMS Collaboration, "Observation of $Z \to 4l$ production in pp collisions at $\sqrt{s}$ = 7 TeV", *CMS Physics Analysis Summary* **CMS-PAS-SMP-12-009 (paper in preparation)** (2012).

[22] CMS Collaboration, "The CMS experiment at the CERN LHC", *JINST* **3** (2008) S08004, doi:10.1088/1748-0221/3/08/S08004.

[23] CMS Collaboration, "Particle-Flow Event Reconstruction in CMS and Performance for Jets, Taus, and MET", CMS Physics Analysis Summary MS-PAS-PFT-09-001, (2009).

[24] CMS Collaboration, "Commissioning of the Particle–Flow reconstruction in Minimum–Bias and Jet Events from pp Collisions at 7 TeV", CMS Physics Analysis Summary CMS-PAS-PFT-10-002, (2010).

[25] S. Baffioni et al., "Electron reconstruction in CMS", *Eur. Phys. J. C* **49** (2007) 1099, doi:10.1140/epjc/s10052-006-0175-5.

[26] CMS Collaboration, "Electron reconstruction and identification at $\sqrt{s} = 7$ TeV", CMS Physics Analysis Summary CMS-PAS-EGM-10-004, (2010).

[27] CMS Collaboration, "Commissioning of the particle-flow event reconstruction with leptons from J/ψ and W decays at 7 TeV", CMS Physics Analysis Summary CMS-PAS-PFT-10-003, (2010).

[28] CMS Collaboration, "Performance of tau-lepton reconstruction and identification in CMS", *JINST* **7** (2012) P01001, arXiv:1109.6034.

[29] M. Cacciari and G. P. Salam, "Pileup subtraction using jet areas", *Phys. Lett. B* **659** (2008) 119, doi:10.1016/j.physletb.2007.09.077, arXiv:0707.1378.

[30] CMS Collaboration, "Measurement of the Inclusive W and Z Production Cross Sections in pp Collisions at $\sqrt{s} = 7$ TeV", *JHEP* **10** (2011) 132, doi:10.1007/JHEP10(2011)132.

[31] S. Frixione, P. Nason, and C. Oleari, "Matching NLO QCD computations with Parton Shower simulations: the POWHEG method", *JHEP* **11** (2007) 070, doi:10.1088/1126-6708/2007/11/070, arXiv:0709.2092.

[32] Y. Gao et al., "Spin determination of single-produced resonances at hadron colliders", *Phys. Rev. D* **81** (2010) 075022, doi:10.1103/PhysRevD.81.075022, arXiv:1001.3396.

[33] T. Sjöstrand, S. Mrenna, and P. Z. Skands, "PYTHIA 6.4 Physics and Manual", *JHEP* **05** (2006) 026, doi:10.1088/1126-6708/2006/05/026, arXiv:hep-ph/0603175.

[34] C. Anastasiou, R. Boughezal, and F. Petriello, "Mixed QCD-electroweak corrections to Higgs boson production in gluon fusion", *JHEP* **04** (2009) 003, doi:10.1088/1126-6708/2009/04/003, arXiv:0811.3458.

[35] D. de Florian and M. Grazzini, "Higgs production through gluon fusion: updated cross sections at the Tevatron and the LHC", *Phys. Lett. B* **674** (2009) 291, doi:10.1016/j.physletb.2009.03.033, arXiv:0901.2427.

[36] J. Baglio and A. Djouadi, "Higgs production at the LHC", *JHEP* **03** (2011) 055, doi:10.1007/JHEP03(2011)055, arXiv:1012.0530.

[37] LHC Higgs Cross Section Working Group, "Handbook of LHC Higgs Cross Sections: 1. Inclusive Observables", CERN Report CERN-2011-002, (2011).

[38] A. Djouadi, M. Spira, and P. M. Zerwas, "Production of Higgs bosons in proton colliders: QCD corrections", *Phys. Lett. B* **264** (1991) 440–446, doi:10.1016/0370-2693(91)90375-Z.

[39] S. Dawson, "Radiative corrections to Higgs boson production", *Nucl. Phys. B* **359** (1991) 283, doi:10.1016/0550-3213(91)90061-2.

[40] M. Spira et al., "Higgs boson production at the LHC", *Nucl. Phys. B* **453** (1995) 17, doi:10.1016/0550-3213(95)00379-7, arXiv:hep-ph/9504378.

[41] R. V. Harlander and W. B. Kilgore, "Next-to-next-to-leading order Higgs production at hadron colliders", *Phys. Rev. Lett.* **88** (2002) 201801, doi:10.1103/PhysRevLett.88.201801, arXiv:hep-ph/0201206.

[42] C. Anastasiou and K. Melnikov, "Higgs boson production at hadron colliders in NNLO QCD", *Nucl. Phys. B* **646** (2002) 220, doi:10.1016/S0550-3213(02)00837-4, arXiv:hep-ph/0207004.

[43] V. Ravindran, J. Smith, and W. L. van Neerven, "NNLO corrections to the total cross section for Higgs boson production in hadron-hadron collisions", *Nucl. Phys. B* **665** (2003) 325, doi:10.1016/S0550-3213(03)00457-7, arXiv:hep-ph/0302135.

[44] S. Catani et al., "Soft-gluon resummation for Higgs boson production at hadron colliders", *JHEP* **07** (2003) 028, doi:10.1088/1126-6708/2003/07/028, arXiv:hep-ph/0306211.

[45] S. Actis et al., "NLO Electroweak Corrections to Higgs Boson Production at Hadron Colliders", *Phys. Lett. B* **670** (2008) 12, doi:10.1016/j.physletb.2008.10.018, arXiv:0809.1301.

[46] M. Ciccolini, A. Denner, and S. Dittmaier, "Strong and electroweak corrections to the production of Higgs + 2-jets via weak interactions at the LHC", *Phys. Rev. Lett.* **99** (2007) 161803, doi:10.1103/PhysRevLett.99.161803, arXiv:0707.0381.

[47] M. Ciccolini, A. Denner, and S. Dittmaier, "Electroweak and QCD corrections to Higgs production via vector-boson fusion at the LHC", *Phys. Rev. D* **77** (2008) 013002, doi:10.1103/PhysRevD.77.013002, arXiv:0710.4749.

[48] T. Figy, C. Oleari, and D. Zeppenfeld, "Next-to-leading order jet distributions for Higgs boson production via weak-boson fusion", *Phys. Rev. D* **68** (2003) 073005, doi:10.1103/PhysRevD.68.073005, arXiv:hep-ph/0306109.

[49] K. Arnold et al., "VBFNLO: A parton level Monte Carlo for processes with electroweak bosons", *Comput. Phys. Commun.* **180** (2009) 1661, doi:10.1016/j.cpc.2009.03.006, arXiv:0811.4559.

[50] P. Bolzoni et al., "Higgs production via vector-boson fusion at NNLO in QCD", *Phys. Rev. Lett.* **105** (2010) 011801, doi:10.1103/PhysRevLett.105.011801, arXiv:1003.4451.

[51] A. Bredenstein et al., "Precise predictions for the Higgs-boson decay H $\to$ WW/ZZ $\to$ 4 leptons", *Phys. Rev. D* **74** (2006) 013004, doi:10.1103/PhysRevD.74.013004, arXiv:hep-ph/0604011.

[52] A. Bredenstein et al., "Radiative corrections to the semileptonic and hadronic Higgs-boson decays H $\to$W W / Z Z$\to$ 4 fermions", *JHEP* **02** (2007) 080, doi:10.1088/1126-6708/2007/02/080, arXiv:hep-ph/0611234.

[53] A. Djouadi, J. Kalinowski, and M. Spira, "HDECAY: A program for Higgs boson decays in the standard model and its supersymmetric extension", *Comput. Phys. Commun.* **108** (1998) 56, doi:10.1016/S0010-4655(97)00123-9, arXiv:hep-ph/9704448.

[54] S. Actis et al., "NNLO Computational Techniques: the Cases $H \to \gamma\gamma$ and $H \to gg$", *Nucl. Phys. B* **811** (2009) 182, doi:10.1016/j.nuclphysb.2008.11.024, arXiv:0809.3667.

[55] J. Alwall et al., "MadGraph/MadEvent v4: The New Web Generation", *JHEP* **09** (2007) 028, doi:10.1088/1126-6708/2007/09/028, arXiv:0706.2334.

[56] T. Binoth, N. Kauer, and P. Mertsch, "Gluon-induced QCD corrections to $pp \to ZZ \to \ell\bar{\ell}\ell'\bar{\ell}'$", in *Proceedings of the XVI Int. Workshop on Deep-Inelastic Scattering and Related Topics (DIS'07)*. 2008. arXiv:0807.0024. doi:10.3360/dis.2008.142.

[57] H.-L. Lai et al., "Uncertainty induced by QCD coupling in the CTEQ global analysis of parton distributions", *Phys. Rev. D* **82** (2010) 054021, doi:10.1103/PhysRevD.82.054021, arXiv:1004.4624.

[58] H.-L. Lai et al., "New parton distributions for collider physics", *Phys. Rev. D* **82** (2010) 074024, doi:10.1103/PhysRevD.82.074024, arXiv:1007.2241.

[59] J. Allison et al., "Geant4 developments and applications", *IEEE Trans. Nucl. Sci.* **53** (2006) 270, doi:10.1109/TNS.2006.869826.

[60] A. Soni and R. Xu, "Probing CP violation via Higgs decays to four leptons", *Phys.Rev.* **D48** (1993) 5259–5263, doi:10.1103/PhysRevD.48.5259, arXiv:hep-ph/9301225.

[61] V. D. Barger, K.-m. Cheung, A. Djouadi et al., "Higgs bosons: Intermediate mass range at e+ e- colliders", *Phys.Rev.* **D49** (1994) 79–90, doi:10.1103/PhysRevD.49.79, arXiv:hep-ph/9306270.

[62] S. Y. Choi, D. J. Miller, M. M. Muhlleitner et al., "Identifying the Higgs spin and parity in decays to Z pairs", *Phys.Lett.* **B553** (2003) 61–71, doi:10.1016/S0370-2693(02)03191-X, arXiv:hep-ph/0210077.

[63] B. Allanach, K. Odagiri, M. Palmer et al., "Exploring small extra dimensions at the large hadron collider", *JHEP* **0212** (2002) 039, arXiv:hep-ph/0211205.

[64] C. P. Buszello, I. Fleck, P. Marquard et al., "Prospective analysis of spin- and CP-sensitive variables in $H \to ZZ \to l(1)^+l(1)^-l(2)^+l(2)^-$ at the LHC", *Eur.Phys.J.* **C32** (2004) 209–219, doi:10.1140/epjc/s2003-01392-0, arXiv:hep-ph/0212396.

[65] R. M. Godbole, D. J. Miller, and M. M. Muhlleitner, "Aspects of CP violation in the H ZZ coupling at the LHC", *JHEP* **0712** (2007) 031, doi:10.1088/1126-6708/2007/12/031, arXiv:0708.0458.

[66] W.-Y. Keung, I. Low, and J. Shu, "Landau-Yang Theorem and Decays of a Z' Boson into Two Z Bosons", *Phys.Rev.Lett.* **101** (2008) 091802, doi:10.1103/PhysRevLett.101.091802, arXiv:0806.2864.

[67] O. Antipin and A. Soni, "Towards establishing the spin of warped gravitons", *JHEP* **0810** (2008) 018, doi:10.1088/1126-6708/2008/10/018, arXiv:0806.3427.

[68] K. Hagiwara, Q. Li, and K. Mawatari, "Jet angular correlation in vector-boson fusion processes at hadron colliders", *JHEP* **0907** (2009) 101, doi:10.1088/1126-6708/2009/07/101, arXiv:0905.4314.

[69] A. De Rujula, J. Lykken, M. Pierini et al., "Higgs look-alikes at the LHC", *Phys.Rev.* **D82** (2010) 013003, doi:10.1103/PhysRevD.82.013003, arXiv:1001.5300.

[70] J. S. Gainer, K. Kumar, I. Low et al., "Improving the sensitivity of Higgs boson searches in the golden channel", *JHEP* **1111** (2011) 027, doi:10.1007/JHEP11(2011)027, arXiv:1108.2274.

[71] J. M. Campbell and R. K. Ellis, "MCFM for the Tevatron and the LHC", *Nucl. Phys. Proc. Suppl.* **205** (2010) 10, doi:10.1016/j.nuclphysbps.2010.08.011, arXiv:1007.3492.

[72] J. M. Campbell and R. K. Ellis, "An update on vector boson pair production at hadron colliders", *Phys. Rev. D* **60** (1999) 113006, doi:10.1103/PhysRevD.60.113006, arXiv:hep-ph/9905386.

[73] J. M. Campbell, R. Ellis, and C. Williams, "Vector boson pair production at the LHC", *JHEP* **07** (2011) 018, doi:10.1007/JHEP07(2011)018, arXiv:1105.0020.

[74] M. Botje et al., "The PDF4LHC Working Group Interim Recommendations", (2011). arXiv:1101.0538.

[75] S. Alekhin et al., "The PDF4LHC Working Group Interim Report", (2011). arXiv:1101.0536.

[76] H.-L. Lai et al., "New parton distributions for collider physics", *Phys. Rev. D* **82** (2010) 074024, doi:10.1103/PhysRevD.82.074024, arXiv:1007.2241.

[77] A. Martin et al., "Parton distributions for the LHC", *Eur. Phys. J. C* **63** (2009) 189, doi:10.1140/epjc/s10052-009-1072-5, arXiv:0901.0002.

[78] R. D. Ball et al., "Impact of Heavy Quark Masses on Parton Distributions and LHC Phenomenology", *Nucl. Phys. B* **849** (2011) 296, doi:10.1016/j.nuclphysb.2011.03.021, arXiv:1101.1300.

[79] CMS Collaboration, "Absolute Calibration of the CMS Luminosity Measurement: Summer 2011 Update", CMS Physics Analysis Summary CMS-PAS-EWK-11-001, (2011).

[80] ATLAS and CMS Collaborations, LHC Higgs Combination Group, "Procedure for the LHC Higgs boson search combination in Summer 2011", ATL-PHYS-PUB/CMS NOTE 2011-11, 2011/005, (2011).

[81] T. Junk, "Confidence level computation for combining searches with small statistics", *Nucl. Instrum. Meth. A* **434** (1999) 435, doi:10.1016/S0168-9002(99)00498-2, arXiv:hep-ex/9902006.

[82] A. Read, "Modified frequentist analysis of search results (the CL_s method)", Technical Report CERN-OPEN-2000-005, CERN, (2000).

[83] Particle Data Group, "Review of particle physics", *J. Phys.* **G37** (2010) 075021, doi:10.1088/0954-3899/37/7A/075021.

[84] M. Oreglia, "A study of the reactions $\psi' \to \gamma\gamma\psi$". PhD thesis, Stanford University, 1980. SLAC-0236.